Bull. Chem. Soc. Ethiop. **2023**, 37(1), 231-244.
DOI: https://dx.doi.org/10.4314/bcse.v37i1.18

ISSN 1011-3924
Printed in Ethiopia
Online ISSN 1726-801X

INVESTIGATION OF LEAD REMOVAL FROM AQUEOUS SOLUTIONS USING MODIFIED NATURAL CLAY: KINETICS AND THERMODYNAMICS APPROACHES

Fatma Ekmekyapar Torun[1*] and Raziye Kısacıkoğlu

Atatürk University, Faculty of Engineering, Environmental Engineering Department, 25240 Erzurum, Turkey

(Received March 1, 2022; Revised August 16, 2022; Accepted August 17, 2022)

ABSTRACT. In this study, the natural clay was modified and removal of Pb^{2+} ions synthetically prepared aqueous solutions using this modified clay was investigated. The parameters affecting the adsorption efficiency were examined in the study. In the result of studies, the suitability of the adsorption data to classic adsorption models, and adsorption kinetics were determined. In the experiments, it has been determined that pH 5 provides optimum removal conditions of adsorption and adsorption reached equilibrium in approximately 15 min. The highest removal efficiency was found to be 82.13% with the addition of 3 g L^{-1} adsorbent at a stirring speed of 200 rpm. As the lead concentration of the wastewater increases, the amount of lead retained per dry unit weight of the modified natural clay also increases. Experimental data showed that Pb^{2+} removal was consistent with Temkin adsorption model. Calculated thermodynamic constants showed that adsorption is exothermic and physical.

KEY WORDS: Adsorption, Isotherm, Lead removal, Natural clay, Thermodynamic constants

INTRODUCTION

Some substances that are not normally found in water, even at very low concentrations, are harmful to human health and can cause illness and even loss of life. Lead, one of the most important of heavy metals, is among these substances [1-6].

Lead is a heavy metal with an atomic number of 82, an atomic weight of 207.2 g mol^{-1}, and a density of 11.34 g cm^{-3}. Lead is very rare in nature but has widespread geography. Lead pollution in wastewaters is most common in metal industries, accumulators, battery factories, oil refineries, paint production industries, and explosive industries [7-10].

Neutralization process, chemical precipitation process, adsorption process, sorption process, ion exchange method, reverse osmosis, and membrane process methods are applied in order to eliminate lead pollution in water [11, 12]. Among these methods, membrane processes and chemical precipitation processes are generally inadequate and expensive in low heavy metal-containing wastewater. Considering that it is always aimed to provide high removal with low cost in engineering applications, it is seen that the most suitable.

Clay minerals have recently been widely used in wastewater treatment [13]. This study, it is aimed to remove lead from aqueous solutions by using modified natural clay. The natural clay mineral used was obtained from the clay quarry located in the Aşkale District of Erzurum Province. In this study where the adsorption method was used, the effects of parameters such as time, pH, temperature, concentration, stirring speed, and adsorbent dosage were examined, and the isotherm constants were determined by investigating the suitability of the results to the adsorption kinetics and equilibrium isotherm equations. In addition, thermodynamic studies were conducted and the values of thermodynamic parameters were determined.

*Corresponding author. E-mail: fyapar@atauni.edu.tr

EXPERIMENTAL

All chemicals used in the study are of analytical purity and the wastewater was prepared synthetically from solid $PbCl_2$. In the experiments, the pH of the wastewater was adjusted using 5 N H_2SO_4 and 5 N NaOH.

The natural clay mineral used in the experiments was obtained cement clay quarry in Aşkale Erzurum, Turkey. The clay to be used for the experiments was grinded in a mortar and brought to certain dimensions, then it was washed with 37% HCl acid solution at certain intervals for 3 days in pure water at a stirring speed of 150 rpm, keeping the pH constant at 4.5. Natural clay samples treated with acid have been modified in this way and brought the pH range suitable for the study. Finally, they were dried in an oven at 100 °C for 48 hours and these dried materials were left in a desiccator for 48 hours. The composition of nature clay and modified clay found by XRF analysis is given in Table 1.

Table 1. Chemical composition of natural clay and modified clay.

Compound	SiO_2	Al_2O_3	Fe_2O_3	CaO	MgO	SO_3	Na_2O	K_2O	L.O.I.	Total
Natural clay (%)	49.21	7.76	5.99	12.41	4.47	0.25	0.41	1.54	15.36	97.4
Modified clay (%)	58.33	10.16	8.59	1.77	4.53	0.26	0.37	1.72	13.86	99.59

The experiments were carried out in Edmund Buhler GmbH Incubator Hood TH brand shaker. Samples were taken at certain time intervals and the Pb^{2+} ion concentrations remaining in the solution were determined by using Shimadzu AA-6800F model atomic adsorption spectrophotometer.

The calculation of the amount of Pb^{2+} adsorbed by the unit modified natural clay (q_e) was made with the equation given in Eq. 1.

$$q_e = \frac{(C_0 - C_e).V}{m} \tag{1}$$

where, q_e is the amount of adsorbed Pb^{2+} ions per unit weight of adsorbent (mg g^{-1}) at equilibrium, C_o and C_e are the initial and equilibrium lead concentrations (mg L^{-1}), V is the volume of the lead solution (L) and m is the modified natural clay mass (g).

Classical adsorption models were used to describe the equilibrium between q_e and C_e at a constant temperature. Freundlich, Langmuir, BET and Temkin isotherm equations used in the experiments are given in Eqs. 2-5, respectively [14-17].

$$logq_e = logK_F + \frac{1}{n}.logC_e \tag{2}$$

$$\frac{1}{q_e} = \frac{1}{a.K_L}.\frac{1}{C_e} + \frac{1}{a} \tag{3}$$

$$\frac{C_e}{(C_s - C_e).q_e} = \frac{1}{K_B.q_s} + .\frac{K_B - 1}{K_B.q_s}.\frac{C_e}{C_s} \tag{4}$$

$$q_e = \frac{R.T}{b_T}.lnK_T + \frac{R.T}{b_T}.lnC_e; B = \frac{R.T}{b_T} \tag{5}$$

where K_F is constant giving the adsorption capacity (mg g^{-1}), n is constant indicating the adsorption intensity (L mg^{-1}), a is maximum adsorption capacity (mg g^{-1}), K_L is constant giving

affinity of the binding sites (L mg^{-1}), C_s is the saturation concentration of the lead (mg L^{-1}), K_B is the constant that gives the energy of interaction with the surface (L mg^{-1}), q_s is amount of lead required to saturate the adsorbent surface (mg g^{-1}), b_T is constant indicating the heat of reaction (J mol^{-1}), K_T is the bonding constant (L g^{-1}), R is the ideal gas constant (8.3145 J mol^{-1} K^{-1}) and T is the temperature (K).

Pseudo first order and pseudo-second order reaction kinetics equations used to determine the reaction degree and rate constants are given in Eqs. 6-7, respectively [18-27].

$$ln\left(q_e - q_t\right) = lnq_e - k_1.t \tag{6}$$

$$\frac{t}{q_t} = \frac{1}{q_e^2.k_2} + \frac{t}{q_e}; q_t = \frac{C_0 - C}{m} \tag{7}$$

where C_0 is the initial Pb^{2+} concentration (mg L^{-1}), C is the Pb^{2+} concentration at any time (mg L^{-1}), q_t is the mg value of the amount of lead adsorbed per gram of modified natural clay at any time (mg g^{-1}), k_1 is the first-order rate constant (min^{-1}), k_2 is the second order rate constant (g mg^{-1} min^{-1}), m is the adsorbent concentration (g L^{-1}), and t is the time (min).

To find the Gibbs free energy in the adsorption process conducted at a certain temperature is given in Eq. 8, to find enthalpy and entropy in the adsorption process is Eq. 9, and activation energy is Eq. 10 [28, 29].

$$\Delta G^\circ = -R.T.lnK_c; K_c = \frac{C_a}{C_e} \tag{8}$$

$$lnK_c = \frac{\Delta S^\circ}{R} - \frac{\Delta H^\circ}{R.T} \tag{9}$$

$$lnk_2 = lnA - \frac{E_a}{R.T} \tag{10}$$

where K_c is the equilibrium constant, C_a is the amount of substance that can be retained in the adsorbent (mg L^{-1}), C_e is the equilibrium concentration of adsorbate (mg L^{-1}), A is the Arrhenius constant, E_a is activation energy (J mol^{-1}).

Adsorbent characterization

SEM, FT-IR, XRD analyses, and zeta measurements were carried out in order to characterize the modified natural clay before and after the adsorption process. FT-IR spectra were obtained using PerkinElmer, Spectrum Two model FT-IR Spectrometer equipped with diamond ATR. FT-IR analyses of adsorbents are used to characterize the bonds between molecules or compounds in the structure and functional groups. Morphological features of the adsorbents were obtained with a Zeiss Sigma 300 Scanning Electron Microscope. All samples were glued to the sample stub and covered with a 10 nm gold-palladium layer for the SEM images. X-Ray diffraction data were obtained using the Bruker D8 Discover XRD device to determine the structural features of adsorbents. Zeta potentials were measured with a zeta-meter (Zeta-Meter 3.0 + 542) for the characterization of colloidal suspensions.

RESULTS AND DISCUSSION

Affecting parameters on lead removal with modified natural clay

The zeta potential measurements of acid-washed clay particles were made in pure water with pH of 2, 3, 4, 5, and 6 and are shown in Figure 1(a). Since the lead ions to be removed began to precipitate converting to $Pb(OH)_2$, which has low solubility above pH 5.5, the zeta potential above this pH was not measured. As a result of the measurements, it was determined that the modified natural clay was negatively loaded at all pH values [30-32]. This enables the negatively charged adsorbent to electrostatically attract positively charged Pb^{2+} ions. Since the negative zeta potential increases at neutral pH, the adsorption efficiency is higher. When the pH is below 4, the H^+ ions in the environment reduce the adsorption efficiency. However, experiments need to be made to determine the amount and conditions of adsorption. The change of q_t versus time at different pH values is given in Figure 1(b).

Studies have shown that q_e values therefore the removal efficiencies decrease significantly when the initial pH of the solution decrease below 4. It can be said that the reason for this is that the concentration of H^+ ions at low pH values is very high and it suppresses the dilute Pb^{2+} ions in water and prevents them from being absorbed. Also, since lead has a large ionic radius (1.20 Å), they have a low charge density and therefore is more affected by the protonation of the surface groups that determine the reduction of the adsorption sites on the clay [33].

In the study of removing lead ions from water by adsorption method using modified natural clay, the effects of adsorbent concentration, Pb^{2+} concentration, adsorbent particle size, and stirring speed on adsorption were investigated after initial pH. The results obtained from experiments are given in Figure 1(c-f). While examining the parameters affecting the adsorption, the parameters examined were changed and 70 mg L^{-1} initial Pb^{2+} concentration, 20 °C temperature, 200 rpm stirring speed, pH 5, and 3 g L^{-1} adsorbent concentration were used.

In studies that examined the effect of adsorbent concentrations, the results obtained showed that the q_e increases until 5 g L^{-1} adsorbent concentration for 70 mg L^{-1} lead concentration. In 5 g L^{-1} adsorbent concentration, the system reaches equilibrium and the q_e values remain approximately constant. From these results, q_e has been determined as 19.16 (mg Pb^{2+} g^{-1}) for 3 g L^{-1} (the removal efficiency was 82.13%) and 12.58 mg Pb^{2+} g^{-1} for 5 g L^{-1} (the removal efficiency was 89.89%) as seen in Figure 1(c).

In studies on lead removal with modified natural clay, the Pb^{2+} ion concentrations were changed between 30-100 mg L^{-1}. The results obtained are given in Figure 1(d). The results show that increasing the adsorbate concentration decreases the q_e value therefore removal efficiency. In addition, as the adsorbate concentration increases, the time to equilibrium also increases.

In the experiments, the effect of different adsorbent sizes on the adsorption efficiency was also examined, and the results are given in Figure 1(e). Even if close results are obtained, it has been determined that the reduction of the adsorbent size increases q_e values therefore the removal efficiency. In the experiments, the highest efficiency was achieved at <0.045 mm particle size. The reason for this is that as the particle size of the adsorbent decreases, the area that the adsorbate can use increases. However, this increase is not very high since the area used in adsorption is the area within the pores rather than the surface area [34, 35].

The experiments made to investigate the effect of stirring speed on adsorption were carried out at 70 mg L^{-1} Pb^{2+}, 3 g L^{-1} adsorbent concentration, 20 °C, and pH 5. The results obtained in the experiments performed at different stirring speeds are shown in Figure 1(f). When Figure 1(f) is examined, it is seen that the time to the equilibrium of adsorption is 60 min at 100 rpm stirring speed, and 15 min at other stirring speeds. When this period is prolonged, it is seen that desorption occurs due to shear forces at 300 rpm and 400 rpm stirring speeds. Since no desorption occurs at 200 rpm stirring speed, the highest q_e value has been obtained. Therefore, it can be said that the optimum stirring speed is 200 rpm. Yang *et al.* and Kofa *et al.* obtained similar results in their studies [36, 37].

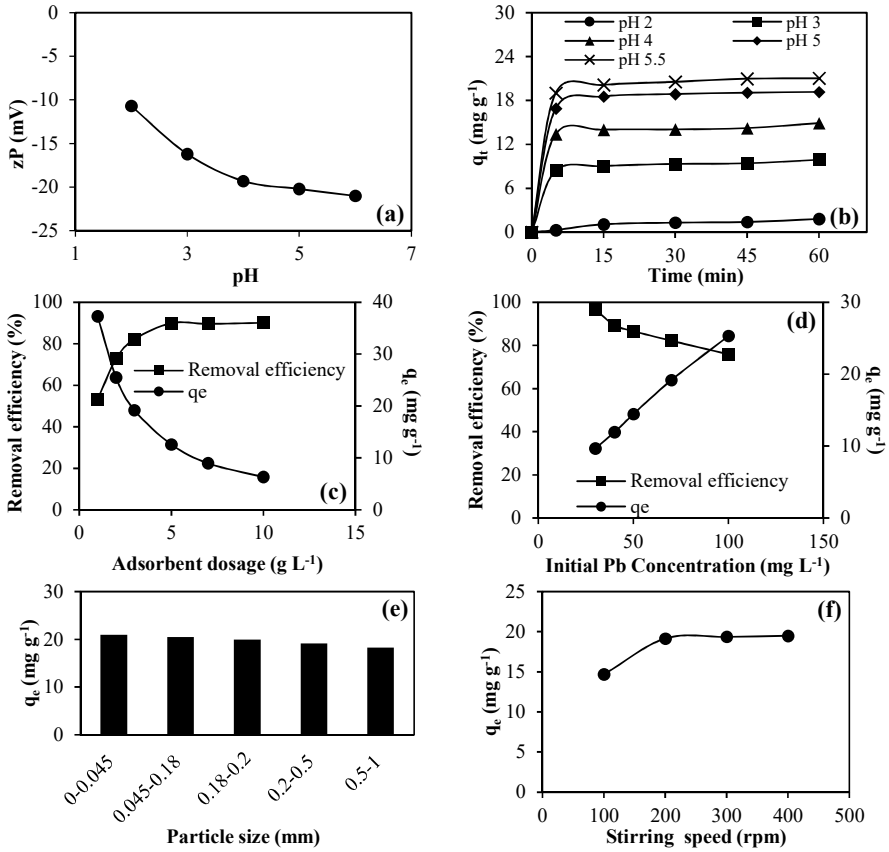

Figure 1. (a) Change of zeta potential of modified natural clay with pH, (b) change of Pb^{2+} removal efficiencies vs time at different initial pHs, (c) the effect of adsorbent concentration on the removal of Pb^{2+} ions, (d) the effect of initial concentration on the removal of Pb^{2+} concentration, (e) the effect of particle size on the removal of Pb^{2+} concentration, and (f) the effect of stirring speed on the removal of Pb^{2+} concentration.

Adsorption kinetics of lead removal reaction with modified natural clay

Pseudo-first order and pseudo-second order kinetic graphs were drawn with the data obtained from studies conducted to examine the effect of temperature. The graphic obtained and the reaction rate constants obtained from these results are shown in Figure 2.

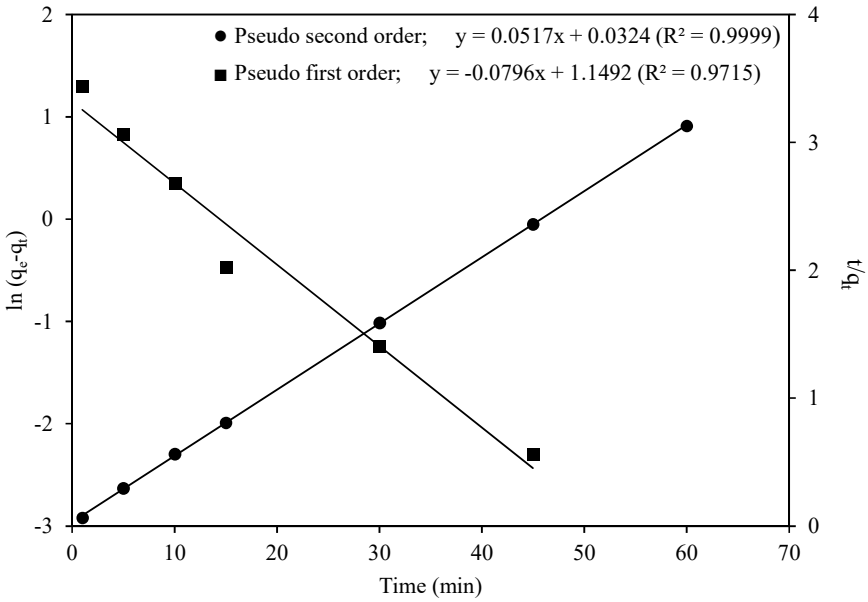

m (g L^{-1})	$q_{e,real}$ (mg g^{-1})	Pseudo first order k_1 (min^{-1})	$q_{e,exp}$ (mg g^{-1})	R^2	Pseudo second order k_2 (gr mg^{-1} min^{-1})	$q_{e,exp}$ (mg g^{-1})	R^2
1	37.262	0.1030	6.019	0.9937	0.0720	34.451	0.9999
2	25.465	0.1185	4.470	0.9477	0.1100	25.575	0.9999
3	19.164	0.0796	3.1557	0.9715	0.1108	19.268	0.9998
5	12.585	0.0973	2.528	0.9702	0.1584	12.658	0.9998
7	8.956	0.0799	1.332	0.9238	0.4866	8.9770	1
10	6.303	0.0509	0.2764	0.7619	1.1660	6.3010	1

Figure 2. Adsorption kinetics of lead removal reaction with modified natural clay for 20 °C pseudo first order and pseudo second order reaction kinetics and reaction rate constants for different adsorbent concentrations.

When Figure 2 is examined, it is seen that the adsorption mechanism of Pb^{2+} removal occurs according to the pseudo-second-order reaction kinetics. Because the q_e values obtained from pseudo-second-order equations are more in agreement with the experimental results. In addition, R^2 values are higher than pseudo-first-order reactions. The pore diffusion plot drawn using the results of the adsorption experiments performed with different Pb^{2+} concentrations is given in Figure 3.

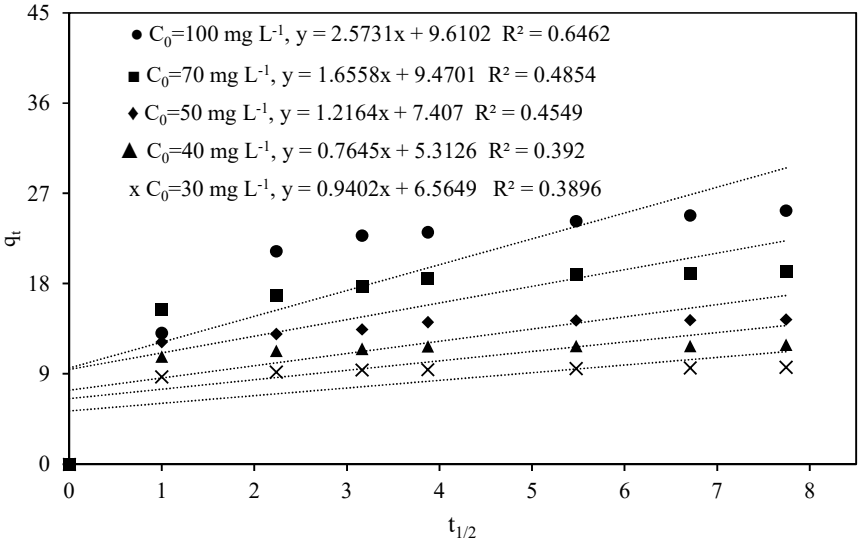

Figure 3. The pore diffusion plot for different Pb^{2+} concentrations.

When Figure 3 is examined, the adsorption is controlled by liquid film diffusion at low Pb^{2+} concentrations. In addition, as the Pb^{2+} concentration increases, the adsorption begins to be controlled by pore diffusion [38]. Pollutants removed in water and wastewater treatment usually consist of dilute solutions. Therefore, adsorption is mostly liquid film controlled. The pore diffusion model is valid because the concentration of the adsorbate will be high if adsorption is used in the recovery and enrichment.

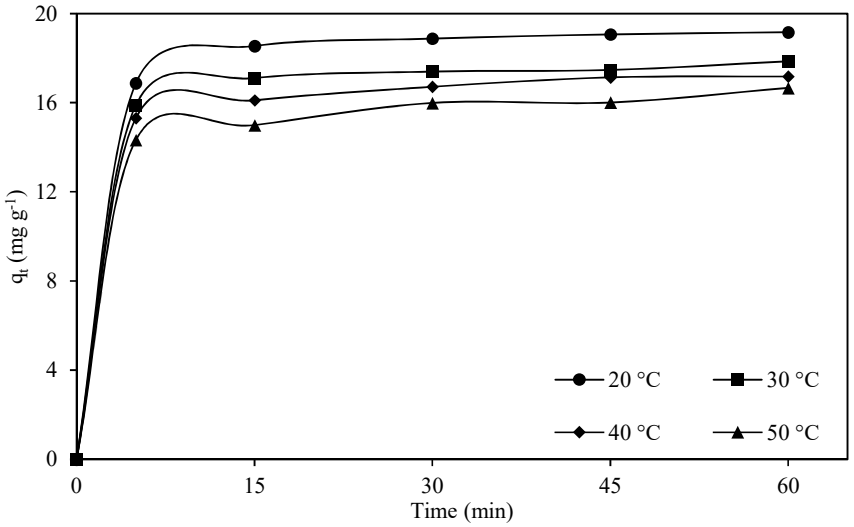

Figure 4. Change of Pb^{2+} removal efficiency versus time at different temperatures in Pb^{2+} removal using modified natural clay.

Effect of temperature on lead adsorption, and thermodynamic parameters calculation

Experiments made to investigate the effect of temperature on adsorption were carried out at 70 mg L^{-1} Pb^{2+} concentration, 3 g L^{-1} adsorbent concentration, 200 rpm stirring speed, and pH 5. The results obtained from the studies conducted at different temperatures are shown in Figure 4.

Experimental data show that the q_e value decreases as the temperature increases. In addition, the desorption phenomenon was observed at high temperatures. Since the adsorption event is an equilibrium reaction, as the temperature increases, the equilibrium concentration increases and the q_e values decrease. This situation indicates that the reaction is an endothermic reaction. As a result of the temperature tests, pseudo-second-order velocity constants and equilibrium constants were calculated and activation energy and thermodynamic constants were found [39]. The graphics drawn for this purpose and the results obtained are given in Figure 5.

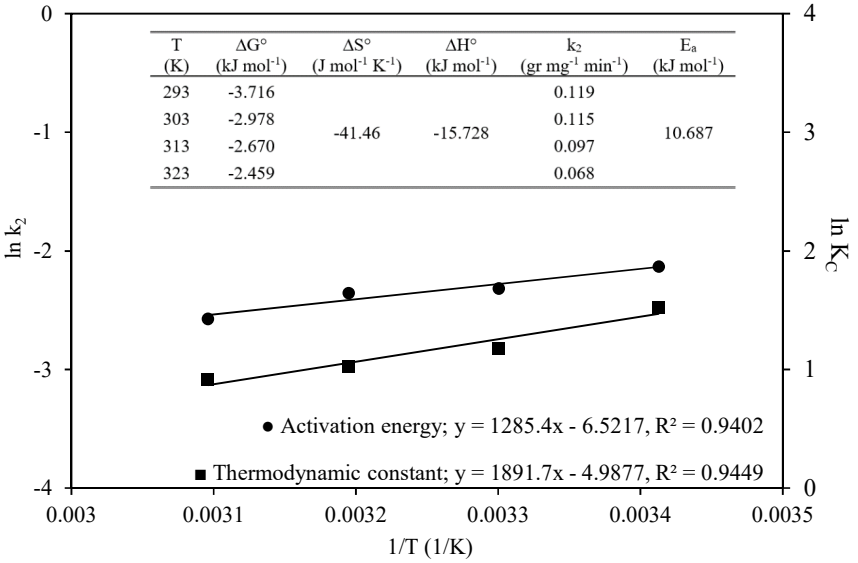

Figure 5. The graphs drawn to find activation energy and thermodynamic constants for Pb^{2+} removal.

In Figure 5, it is seen that ΔG° values are negative at all the temperatures and decreases with increasing temperature. The negative Gibbs free energy indicates that the reaction proceeds spontaneously, and the decrease of ΔG° as the temperature increases indicates also more spontaneous at low temperatures. Negative ΔH° indicates that adsorption is an exothermic reaction and negative ΔS° value indicates that adsorption is not random [40]. If the activation energy is between 5 kJ mol^{-1} and 40 kJ mol^{-1}, adsorption is defined as physical adsorption [41]. When the activation energy is examined, it can be said that adsorption is physical adsorption and occurs rapidly.

Adsorption isotherms of lead removal reaction with modified natural clay

Calculations of isotherms were carried out with the data obtained from the studies made to examine the effect of the amount of adsorbent. Freundlich, Langmuir, BET, and Temkin isotherms curves were drawn according to the results obtained from these curves and the isotherm coefficients are given in Figure 6.

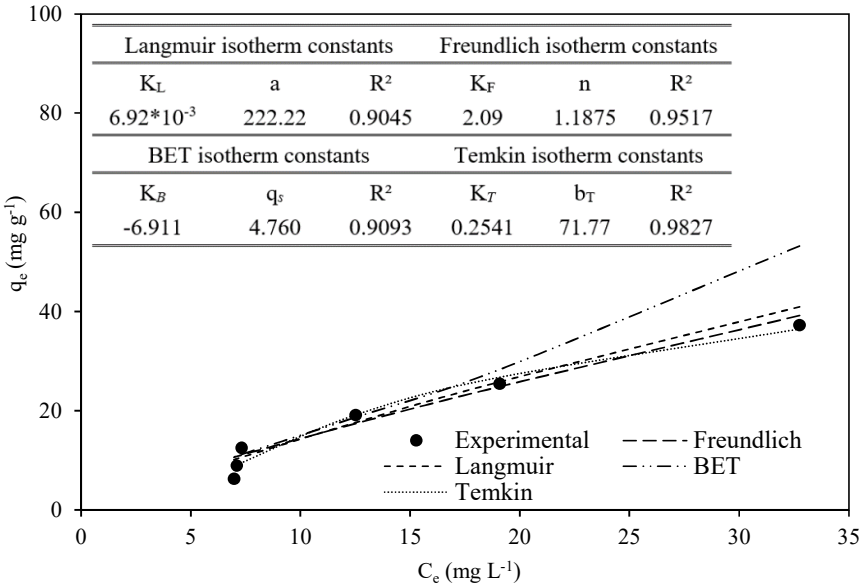

Figure 6. Langmuir, Freundlich, BET, and Temkin isotherm curves.

When Figure 6 is examined, it can be said that the adsorption is more suitable for Temkin isotherm than the others.

Adsorbent characterization

As a result of adsorption studies, modified natural clay samples taken before and after adsorption were subjected to EDX, XRD, FT-IR and SEM imaging. EDX spectra of the samples taken are given in Figure 7(a-b) and XRD, FT-IR and SEM images are given in Figure 7(c-f).

While there are high levels of Si, Ca, Al, Fe, Mg and O in the natural clay, other substances are found in trace amounts. Before the natural clay was modified, the CaO compound in its structure was dissolved in water, causing the pH of the water to rise. At the end of the modification, some amount of CaO was transferred to water, preventing the increase of pH during adsorption. It was determined that the amount of some substances decreased in the modified natural clay after adsorption. Adsorption of Pb^{2+} on the adsorbent was confirmed by EDX analysis. It was determined that as the Pb^{2+} content on the adsorbent increased, the Ca, Mg, S and O contents decreased. The amount of O, which was 33.35% before the adsorption, decreased to 22.62% after adsorption. The Ca content from 1.77% to 0, the Mg content from 3.4% to 2.76% decreased. Besides, Pb amount increased from 0% to 3.94%. As can be understood from here, Pb^{2+} ions bind to instead of SiO_2, MgO and CaO ions [42].

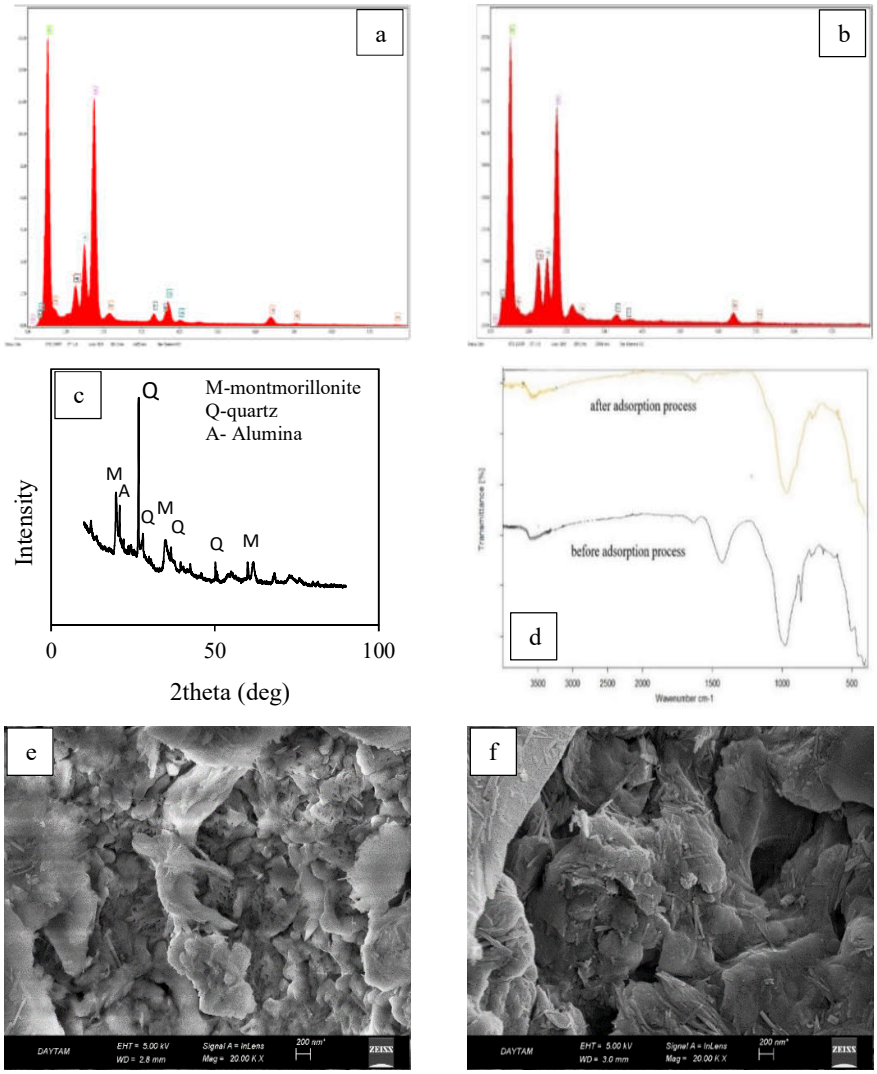

Figure 7. (a) EDX spectra of modified natural clay before adsorption, (b) EDX spectra of modified natural clay after adsorption, (c) XRD diagram of natural clay, (d) FT-IR images before and after lead removal, (e) SEM images before the experiments, (f) SEM images after lead removal

According to the EDX results, the elemental composition of the adsorbent before and after the experiment is given in Table 2. When Figure 7(a) is examined, it is seen that natural clay is mostly composed of calcite-montmorillonite-alumina. Further, the occurrence of the above minerals in the adsorbents was confirmed by the FT-IR study. Significant IR bands of modified and raw clay are given in Table 3. In addition, the sharp peaks formed indicate that the natural clay has a largely inhomogeneous crystalline structure.

Table 2. Elemental composition of natural and modified clay before and after adsorption.

Compounds	Natural clay weight (%)	Modified clay weight (%)	After adsorption weight (%)
O	45.65	33.35	22.62
Mg	3.55	3.40	2.76
Al	9.14	8.23	7.21
Si	22.99	18.45	16.87
K	1.66	1.22	1.17
Ca	8.2	1.77	could not be measured
Fe	8.62	5.71	5.43
Pb			3.94

Table 3. Significant IR bands of modified and raw clay.

Wavelength (cm^{-1})	Raw clay (%T)	Modified clay (%T)	After experiments (%T)	Assignments
511	49.115	47.76	59.28	Si-O str., Si-O-Al stretching
810	77.35	77.335	84.50	Si-O str., Si-O-(Al-Mg)
888	-	60.5	-	Deformation of OH linked to Fe^{3+} and Al^{3+}
989	44.11	42.3	54.066	Si-O planar stretching
1466	-	75.515	-	H-O-H bending
1666	92.341	92.35	95.68	H-O-H stretching
3611	87.335	85.523	93.19	Inner layer OH(Al-O-H)

When Table 3 is examined, the adsorption characteristic of Pb^{2+} ions in combination with stretching vibrations of Si-O bonds appear in the region of 1281-841 cm^{-1} [43]. The bands from 1708 cm^{-1} to 1576 cm^{-1} correspond to the O-H bending vibrations of H_2O molecules [44]. Stretching vibrations of Fe-O bonds appear in the region of 648-515 cm^{-1}. The overlapping bands in the region from 3660 cm^{-1} to 3120 cm^{-1} correspond to the stretching vibrations of Al-OH groups and O-H bonds under hydrogen bonded groups [45].

When the FT-IR images given in Figure 7(d) are examined, two peaks that are not particularly in raw clay and disappeared in modified clay after the experiment draw attention. These peaks are visible at 888 cm^{-1} and 1466 cm^{-1} wavelengths. Both peaks represent the O-H degradation that is produced as a result of washing with acid. When Table 3 is examined, Si-O stretching vibrations of 511 cm^{-1}, 711 cm^{-1}, 810 cm^{-1}, and 989 cm^{-1} wavelengths indicating the presence of quartz were obtained. Peaks at 888 cm^{-1} wavelengths show the decay of OH connected to Fe and Al, and the 3611 cm^{-1} band shows Al-O-H inner layer stress. The 1666 cm^{-1} band indicates the presence of H-O-H stretching vibration. 1466 cm^{-1} shows the H-O-H bending stress [46].

The SEM images given in Figure 7(e) and Figure 7(f) show that the porous structure of clay is not homogeneous. SEM images show different structural features with an uneven surface. After adsorption, the adsorbed molecules remained as aggregates on the clay surface.

CONCLUSION

In this study, parameters affecting the adsorption of Pb^{2+} ions with modified natural clay from synthetically prepared wastewaters were investigated and optimum conditions for maximum adsorption were determined.

Studies to determine the effect of pH were carried out between pH 2-5.5, because when pH > 6, Pb^{2+} ions begin to precipitate by forming $Pb(OH)_2$. Studies show that the adsorption efficiency is less at low pH and the removal efficiency increases as it approaches neutral pH. The zeta potential of modified natural clay at neutral pH's reaching maximum values negatively and its adsorption with electrostatic attraction forces explain this high removal efficiency.

Studies have shown that increasing the adsorbent concentration increases the removal efficiency, but the removal efficiency remains constant after a certain concentration. This adsorbent dosage, where the adsorbent surface area is used optimally, was determined as 5 g L^{-1} for 70 mg L^{-1} Pb^{2+} concentration. Again, in studies conducted for the effect of stirring speed, the efficiency was low due to insufficient contact between the adsorbent and the adsorbate at low stirring speeds, and desorption occurred due to shear forces at high stirring speeds. In studies investigating the effect of particle size, it can be said that particle size does not have much effect, but the removal efficiency increases as the particle size decrease, albeit a little.

Then, kinetic studies were conducted and the reaction degree was determined by applying the obtained data to pseudo-first-order and pseudo-second-order kinetics. As a result of the calculations, it was concluded that the lead adsorption reaction proceeds according to the pseudo-second-order kinetic equation. According to the pseudo-second degree, the reaction rate constant at 20 ºC was determined as 0.1187 g mg^{-1} min^{-1}.

As a result of temperature studies, it was observed that the adsorption rate of Pb^{2+} adsorption decreased slightly with the increase in temperature and its efficiencies of removal decreased slightly. Reaction rate constants, equilibrium constants, and activation energy were calculated at the end of the studies that investigated the effect of temperature. As a result of these investigations, for Pb^{2+} adsorption, as the reaction enthalpy $\Delta H°$ = -15.728 kJ mol^{-1}, reaction entropy as $\Delta S°$ = -41.46 J mol^{-1} K^{-1} were determined. If $\Delta H°$ is negative, the reaction is exothermic, and if $\Delta G°$ is negative, indicating that adsorption occurs spontaneously. The negative $\Delta S°$ indicates that the randomness is low. The activation energy of the reaction was found to be 10.687 kJ mol^{-1}. This shows that Pb^{2+} adsorption is physical adsorption.

Before and after adsorption XRD, SEM and FT-IR imaging were performed to determine the characterization of modified natural clay. As a result of these, it has been determined that sewage sludge ash has a porous, irregular and high crystal structure.

As a result, it can be said that the adsorption process, which is a preferred method based on the principle of removing a pollutant with a substance abundant in nature, without any harm to our environment, can be easily used in the treatment of industrial wastewater containing lead.

REFERENCES

1. Yu, B.; Zhang, Y.; Shukla, A.; Shukla, S.S.; Dorris, K.L. The removal of heavy metals from aqueous solutions by sawdust adsorption — removal of lead and comparison of its adsorption with copper. *J. Hazard. Mater.* **2001**, 84, 83-94.
2. Rahman, Z.; Singh, V.P. The relative impact of toxic heavy metals (THMs) (arsenic (As), cadmium (Cd), chromium (Cr) (VI), mercury (Hg), and lead (Pb)) on the total environment: An overview. *Environ. Monit. Assess.* **2019**, 191, 419.
3. Lakherwal, D. Adsorption of heavy metals: A review. *Int. J. Environ. Res. Dev.* **2014**, 4, 41-48.
4. Rocha, A.; Trujillo, K.A. Neurotoxicity of low-level lead exposure: History, mechanisms of action, and behavioral effects in humans and preclinical models. *Neurotoxicology* **2019**, 73, 58-80.
5. Kul, S.; Gül, V.; Cengiz, İ. Investigation of heavy metal pollution in soil and plants: The case of Bayburt province. *Journal of Anatolian Environmental and Animal Science (JAES)* **2021**, 6, 195-203.
6. Gül, V.; Kul, S. Determination of some heavy metals in oil sunflower seeds grown in the north of Turkey. *Eur. J. Sci. Technol.* **2021**, 23, 725-729.
7. Citak, D.; Tuzen, M. A novel preconcentration procedure using cloud point extraction for determination of lead, cobalt and copper in water and food samples using flame atomic absorption spectrometry. *Food Chem. Toxicol.* **2010**, 48, 1399-1404.

8. Adebisi, G.A.; Chowdhury, Z.; Alaba, P.A. Equilibrium, kinetic, and thermodynamic studies of lead ion and zinc ion adsorption from aqueous solution onto activated carbon prepared from palm oil mill effluent. *J. Clean. Prod.* **2017**, 148, 958-968.
9. Khulbe, K.C.; Matsuura, T. Removal of heavy metals and pollutants by membrane adsorption techniques. *Appl. Water Sci.* **2018**, 8, 19.
10. Awual, R. An efficient composite material for selective lead(II) monitoring and removal from wastewater. *J. Environ. Chem. Eng.* **2019**, 7, 103087.
11. Arbabi, M.; Hemati, S.; Amiri, M. Removal of lead ions from industrial wastewater: A review of Removal methods. *Int. J. Epidemiol. Res.* **2015**, 2, 105-109.
12. Attia, H.; Alexander, S.; Wright, C.J.; Hilal, N. Superhydrophobic electrospun membrane for heavy metals removal by air gap membrane distillation (AGMD). *Desalination* **2017**, 420, 318-329.
13. Farizoglu, B.; Fil, B.A.; Sozudogru, O.; Aladag, E.; Kul, S. Comparison of cationic dyes (basic orange 2, basic yellow 2 and basic violet 3) removal from aqueous solution using clay as an adsorbent. *Fresenius Environ. Bull.* **2019**, 28, 3658-3666.
14. Freundlich, H.M.F. Uber die adsorption in losungen. *Zeitschrift fr Physikalische Chemie.* **1907**, 57, 385-470.
15. Langmuir, I. The adsorption of gases on plane surfaces of glass, mica and platinum. *J. Am. Chem. Soc.* **1918**, 40, 1361-1403.
16. Brunauer, S.; Emmett, P.H.; Teller, E. Adsorption of gases in multimolecular layers. *J. Am. Chem. Soc.* **1938**, 60, 309-319.
17. Temkin, M.; Pyzhev, V., Kinetics of ammonia synthesis on promoted iron catalysts. *Acta Physicochimica URSS* **1940**, 12, 327-356.
18. Kul, S. Removal of Cu(II) from aqueous solutions using modified sewage sludge ash. *Int. J. Environ. Sci. Technol.* **2021**, 18, 3795–3806.
19. Mahmoud, D.K.; Salleh, M.A.M.; Karim, W.A.W.A.; Idris, A.; Abidin, Z.Z. Batch adsorption of basic dye using acid treated kenaf fibre char: Equilibrium, kinetic and thermodynamic studies. *Chem. Eng. J.* **2012**, 181-182, 449-457.
20. Hameed, B.H.; Ahmad, A.L.; Latiff, K.N.A. Adsorption of basic dye (methylene blue) onto activated carbon prepared from rattan sawdust. *Dyes Pigm.* **2007**, 75, 143-149.
21. Franca, A.S.; Oliveira L.S.; Ferreira, M.E. Kinetics and equilibrium studies of methylene blue adsorption by spent coffee grounds. *Desalination* **2009**, 249, 267-272.
22. Agarwal, S.; Tyagi, I.; Gupta, V.K.; Ghasemi, N.; Shahivand, M.; Ghasemi, M. Kinetics, equilibrium studies and thermodynamics of methylene blue adsorption on Ephedra strobilacea saw dust and modified using phosphoric acid and zinc chloride. *J. Mol. Liq.* **2016**, 208, 208-218.
23. Bingul, Z. Determination of affecting parameters on removal of methylene blue dyestuff from aqueous solutions using natural clay: Isotherm, kinetic, and thermodynamic studies. *J. Mol. Struct.* **2022**, 1250, 131729.
24. Reçber, Z. Adsorption of methylene blue onto spent *Alchemilla vulgaris* leaves: Characterization, isotherms, kinetic and thermodynamic studies. *Int. J. Environ. Sci. Technol.* **2022**, 19, 4803-4814.
25. İrdemez, Ş.; Durmuş, G.; Kul, S.; Ekmekyapar Torun, F.; Bingül, Z. Comparison of kinetics of Cr(III) ions removal from wastewater using raw and activated montmorillonite minerals. *J. Environ. Qual.* **2021**, 45, 17-26.
26. İrdemez, Ş.; Yeşilyurt, D.; Ekmekyapar Torun, F.; Kul, S.; Bingül, Z. Investigation of manganese ions removal from waters using sewage sludge ash. *Iran J. Chem. Chem. Eng.* **2021**. DOI: 10.30492/IJCCE.2021.527060.4639.
27. Ekmekyapar Kul, Z.; Nuhoğlu, Y.; Kul, S.; Nuhoğlu, Ç.; Ekmekyapar Torun, F. Mechanism of heavy metal uptake by electron paramagnetic resonance and FTIR: Enhanced manganese(II) removal onto waste acorn of *Quercus ithaburensis*. *Sep. Sci. Technol.* **2016**, 51, 115-125.

28. Sözüdoğru, O.; Fil, B.A.; Boncukcuoğlu, R.; Aladağ, E.; Kul, S. Adsorptive removal of cationic (BY2) dye from aqueous solutions onto Turkish clay: Isotherm, kinetic, and thermodynamic analysis. *Part. Sci. Technol.* **2016**, 34, 103-111.
29. Nuhoğlu, Y.; Ekmekyapar Kul, Z.; Kul, S.; Nuhoğlu, Ç.; Ekmekyapar Torun, F. Pb(II) biosorption from the aqueous solutions by raw and modified tea factory waste (TFW). *Int. J. Environ. Sci. Technol.* **2021**, 18, 2975-2986
30. Yukselen, Y.; Kaya, A. Zeta potential of kaolinite in the presence of alkali, alkaline earth and hydrolyzable metal ions. *Water Air Soil Pollut.* **2003**, 145, 155-168.
31. Vane, L.M.; Zang, G.M. Effect of aqueous phase properties on clay particle zeta potential and electro-osmotic permeability: Implications for electro-kinetic soil remediation processes. *J. Hazard. Mater.* **1997**, 55, 1-22.
32. Liu, J.; Zhou, Z.; Xu, Z.; Masliyah, J. Bitumen–clay interactions in aqueous media studied by zeta potential distribution measurement. *J. Colloid Interface Sci.* **2002**, 252, 409-418.
33. Abollino, O.; Aceto, M.; Malandrino, M.; Sarzanini, C.; Mentasti, E. Adsorption of heavy metals on Na-montmorillonite. Effect of pH and organic substances. *Water Res.* **2003**, 7, 1619-1627.
34. Kumar, P.S.; Korving, L.; Keesman, K.J.; Van Loosdrecht, M.C.M.; Witkamp, G-J. Effect of pore size distribution and particle size of porous metal oxides on phosphate adsorption capacity and kinetics. *Chem. Eng. J.* **2019**, 358, 160-169.
35. Ayuba, S.; Mohammadib, A.A.; Yousefic, M.; Changanic, F. Performance evaluation of agro-based adsorbents for the removal of cadmium from wastewater. *Desalination Water Treat.* **2019**, 142, 293-299.
36. Yang, Y.; Ding, Q.; Yang, M.; Wang, Y.; Zhang, X. Magnetic ion exchange resin for effective removal of perfluorooctanoate from water: study of a response surface methodology and adsorption performances. *Environ. Sci. Pollut. Res.* **2018**, 25, 29267-29278.
37. Kofa, G.P.; Gomdje, V.H.; Telegang, C.; Koungou, S. Removal of fluoride from water by adsorption onto fired clay pots: Kinetics and equilibrium studies. *J. Appl. Chem.* **2017**, 6254683.
38. Weber, W.J.; Morris, J.C. Kinetics of adsorption on carbon from solution. *J. Sanit. Eng. Div.* **1963**, 89, 31-60.
39. Konicki, W.; Aleksandrzak, M.; Mijowska, E. Equilibrium, kinetic and thermodynamic studies on adsorption of cationic dyes from aqueous solutions using graphene oxide. *Chem. Eng. Res. Des.* **2017**, 123, 35-49.
40. Lima, E.C.; Hosseini-Bandegharaei, A.; Moreno-Piraján, J.C.; Anastopoulos, I. A critical review of the estimation of the thermodynamic parameters on adsorption equilibria. Wrong use of equilibrium constant in the Van't Hoof equation for calculation of thermodynamic parameters of adsorption. *J. Mol. Liq.* **2019**, 273, 425-434.
41. Wu, C. Adsorption of reactive dye onto carbon nanotubes: Equilibrium, kinetics and thermodynamics. *J. Hazard. Mater.* **2007**, 144, 93-100.
42. Wang, Q.; Li, J.; Poon, C.S. Using incinerated sewage sludge ash as a high-performance adsorbent for lead removal from aqueous solutions: Performances and mechanisms. *Chemosphere* **2019**, 226, 587-596.
43. Nayak, P.S.; Singh, B.K. Instrumental characterization of clay by XRF, XRD and FTIR. *Bull. Mater. Sci.* **2007**, 30, 235-238.
44. Aroke, U.O.; El-Nafaty, U.A. XRF, XRD and FTIR Properties and characterization of HDTMA-Br surface modified organo-kaolinite clay. *Int. J. Emerging Technol. Adv. Eng.* **2014**, 4, 817-825.
45. Chen, P.; Culbreth, M.; Aschner, M. Exposure, epidemiology, and mechanism of the environmental toxicant manganese. *Environ. Sci. Pollut. Res.* **2016**, 23, 13802-13810.
46. Sarı, A. Composites of polyethylene glycol (PEG600) with gypsum and natural clay as new kinds of building PCMs for low temperature-thermal energy storage. *Energy Build.* **2014**, 69, 184-192.